

Observability of 2HDM neutral Higgs bosons with different masses at future e^+e^- linear colliders

Majid Hashemi and Gholamhossein Haghightat

*Physics Department, College of Sciences, Shiraz University,
Shiraz, 71946-84795, Iran*

E-mail: hashemi_mj@shirazu.ac.ir, hosseinhaqiqat@gmail.com

ABSTRACT: Assuming two Higgs doublet model (2HDM) at SM-like scenario as the theoretical framework, this study addresses the question of observability of heavy neutral CP-even and CP-odd Higgs bosons H and A at a linear collider operating at $\sqrt{s} = 1$ TeV. The signal production channel is $e^-e^+ \rightarrow AH \rightarrow ZHH$ with subsequent leptonic decay of the Z boson and Higgs bosons decays into b quark pairs. Therefore, to be specific, type-I 2HDM is used to allow dominant Higgs boson decay to b -quark pairs below the top quark pair production threshold. Two benchmark points with mass ranges $150 \leq m_H \leq 200$ and $250 \leq m_A \leq 300$ are simulated. The relevant energy and momentum smearing is applied and appropriate selection cuts are imposed to enrich signal events. Results indicate that both Higgs bosons are observable with signals exceeding 5σ significance with possibility of mass measurement at the integrated luminosity of 500 fb^{-1} .

Contents

1	Introduction	1
2	Two-Higgs-doublet model	2
3	Signal process	4
4	Analysis	6
5	Higgs boson reconstruction	9
6	Signal significance	13
7	Conclusions	13

1 Introduction

The standard model (SM) of elementary particles has been verified by many experiments and played an important role in understanding a wide range of phenomena. Existence of the Higgs boson [1–6] as one of the most important predictions of the standard model was verified experimentally [7, 8] and triggered an increasing interest in studying SM extensions. Extensions of the SM are also motivated by supersymmetry [9], axion models [10], the SM inability to explain the universe baryon asymmetry [11], etc. The standard model uses the simplest possible scalar structure with one $SU(2)$ Higgs doublet. Such an assumption leads to the prediction of a single Higgs boson. However, employing two $SU(2)$ Higgs doublets leads to a kind of SM extension which may resolve the present unsolved problems of the physics.

As one of the simplest extensions of the standard model, two-Higgs-doublet model (2HDM) [12–19] has emerged as an important candidate which predicts five Higgs bosons, four of which are assumed to be, yet undiscovered, Higgs bosons and the fifth one (the lightest one) is assumed to be the same as the observed SM Higgs boson. Prediction of the existence of five Higgs bosons is a direct consequence of assuming two $SU(2)$ Higgs doublets in this model. Two out of the four undiscovered Higgs bosons are neutral scalar and pseudoscalar Higgs bosons H and A , and the others are charged Higgs bosons H^\pm . This paper focuses on the neutral Higgs bosons H and A in the context of the Type-I 2HDM at SM-like scenario and addresses the question of observability of these Higgs bosons at a linear collider operating at the center-of-mass energy of $\sqrt{s} = 1$ TeV. Type-I 2HDM is one of the four types of the 2HDM which naturally conserve flavor and are derived from imposing the discrete Z_2 symmetry.

In this study, the process $e^-e^+ \rightarrow AH \rightarrow ZHH \rightarrow \ell\bar{\ell}b\bar{b}b\bar{b}$, where $\ell\bar{\ell}$ is an electron or a muon pair, is assumed as the signal process. The decay mode $H \rightarrow b\bar{b}$ is motivated at high $\tan\beta$ by the significant enhancement compared to other modes. This is due to the fact that Higgs-fermion couplings are proportional to the same $\cot\beta$ factor which is canceled out when branching ratios of Higgs boson decays are calculated. Therefore as long as the Higgs boson mass is below the on-shell production of the top quark pair production, $H \rightarrow b\bar{b}$ remains dominant. Despite having a small branching ratio (≈ 0.066), the decay mode $Z \rightarrow e^-e^+$ or $\mu^-\mu^+$ is chosen for signal to benefit from the clear signature electrons and muons provide at linear colliders.

To investigate the observability of the signal, two benchmark points in the parameter space of the Type-I 2HDM are assumed to search for heavy neutral CP-even and CP-odd Higgs bosons H and A with the help of appropriate selection cuts. We finally try to reconstruct masses of the Higgs bosons. Results indicate that, for both benchmark points, the Higgs bosons H and A are observable at a 1 TeV collider with 5σ signals at integrated luminosities 46 and 112 fb^{-1} respectively.

In what follows, we provide a brief introduction to the 2HDM and its flavor conserving types, and then the signal and background analysis and results will be provided.

2 Two-Higgs-doublet model

A general 2HDM assumes the Higgs potential to be

$$\begin{aligned} \mathcal{V} = & m_{11}^2 \Phi_1^\dagger \Phi_1 + m_{22}^2 \Phi_2^\dagger \Phi_2 - \left[m_{12}^2 \Phi_1^\dagger \Phi_2 + \text{h.c.} \right] \\ & + \frac{1}{2} \lambda_1 \left(\Phi_1^\dagger \Phi_1 \right)^2 + \frac{1}{2} \lambda_2 \left(\Phi_2^\dagger \Phi_2 \right)^2 + \lambda_3 \left(\Phi_1^\dagger \Phi_1 \right) \left(\Phi_2^\dagger \Phi_2 \right) + \lambda_4 \left(\Phi_1^\dagger \Phi_2 \right) \left(\Phi_2^\dagger \Phi_1 \right) \quad (2.1) \\ & + \left\{ \frac{1}{2} \lambda_5 \left(\Phi_1^\dagger \Phi_2 \right)^2 + \left[\lambda_6 \left(\Phi_1^\dagger \Phi_1 \right) + \lambda_7 \left(\Phi_2^\dagger \Phi_2 \right) \right] \left(\Phi_1^\dagger \Phi_2 \right) + \text{h.c.} \right\}, \end{aligned}$$

where Φ_1 and Φ_2 are $SU(2)$ Higgs doublets. Employing the extended scalar structure with two Higgs doublets leads to the prediction of three neutral Higgs bosons h , H and A , and two charged Higgs bosons H^\pm . h and H are scalar CP-even bosons and A is a pseudoscalar CP-odd boson. Working in the ‘‘physical basis’’, physical Higgs masses, $\tan\beta$, CP-even Higgs mixing angle α , m_{12}^2 , λ_6 and λ_7 are parameters of the model and must be determined [12]. m_{11}^2 and m_{22}^2 in the Higgs potential 2.1 are determined by the minimization conditions for a minimum of the vacuum once $\tan\beta$ is determined. Imposing discrete Z_2 symmetry [14–16] to avoid tree level flavor-changing neutral currents (FCNC) implies that the values of the parameters λ_6 , λ_7 and m_{12}^2 must be zero. However, setting λ_6 , λ_7 to zero and allowing a non-zero value for m_{12}^2 , Z_2 symmetry is softly broken in 2HDM. Imposing Z_2 symmetry restricts Higgs coupling to fermions and implies that there are four types of the 2HDM which naturally conserve flavour. Table 1 shows how Higgs doublets couple to fermions in different types. The types ‘‘X’’ and ‘‘Y’’ are also called ‘‘lepton-specific’’ and ‘‘flipped’’ respectively. Applying the coupling prescription of table 1, Higgs-fermion interaction part

	u_R^i	d_R^i	ℓ_R^i
Type I	Φ_2	Φ_2	Φ_2
Type II	Φ_2	Φ_1	Φ_1
Type X	Φ_2	Φ_2	Φ_1
Type Y	Φ_2	Φ_1	Φ_2

Table 1: Higgs coupling to up-type quarks, down-type quarks and leptons in different types. The superscript i is a generation index.

of the Lagrangian becomes [12]

$$\begin{aligned}
\mathcal{L}_{Yukawa} = & - \sum_{f=u,d,\ell} \frac{m_f}{v} \left(\xi_h^f \bar{f} f h + \xi_H^f \bar{f} f H - i \xi_A^f \bar{f} \gamma_5 f A \right) \\
& - \left\{ \frac{\sqrt{2} V_{ud}}{v} \bar{u} (m_u \xi_A^u P_L + m_d \xi_A^d P_R) d H^+ + \frac{\sqrt{2} m_\ell \xi_A^\ell}{v} \bar{\nu}_L \ell_R H^+ + H.c. \right\}.
\end{aligned} \tag{2.2}$$

Table 2 provides ξ_Y^X factors corresponding to different types. In order to respect experi-

	I	II	X	Y
ξ_h^u	c_α/s_β	c_α/s_β	c_α/s_β	c_α/s_β
ξ_h^d	c_α/s_β	$-s_\alpha/c_\beta$	c_α/s_β	$-s_\alpha/c_\beta$
ξ_h^ℓ	c_α/s_β	$-s_\alpha/c_\beta$	$-s_\alpha/c_\beta$	c_α/s_β
ξ_H^u	s_α/s_β	s_α/s_β	s_α/s_β	s_α/s_β
ξ_H^d	s_α/s_β	c_α/c_β	s_α/s_β	c_α/c_β
ξ_H^ℓ	s_α/s_β	c_α/c_β	c_α/c_β	s_α/s_β
ξ_A^u	$\cot \beta$	$\cot \beta$	$\cot \beta$	$\cot \beta$
ξ_A^d	$-\cot \beta$	$\tan \beta$	$-\cot \beta$	$\tan \beta$
ξ_A^ℓ	$-\cot \beta$	$\tan \beta$	$\tan \beta$	$-\cot \beta$

Table 2: ξ_Y^X factors corresponding to different types ($c_x \equiv \cos x$ and $s_x \equiv \sin x$).

mental observations, it is assumed that the lightest Higgs boson h predicted by the 2HDM is the same as the discovered SM Higgs boson and thus the SM-like scenario is chosen by assuming $\sin(\beta - \alpha) = 1$ [12]. Therefore the h -fermion couplings of the Yukawa Lagrangian of the 2HDM reduce to the corresponding couplings of the standard model. As a result,

the neutral Higgs part of the Yukawa Lagrangian takes the form [20]

$$\begin{aligned}
\mathcal{L}_{Yukawa} = & -v^{-1} \left(m_d \bar{d}d + m_u \bar{u}u + m_\ell \bar{\ell}\ell \right) h \\
& + v^{-1} \left(\rho^d m_d \bar{d}d + \rho^u m_u \bar{u}u + \rho^\ell m_\ell \bar{\ell}\ell \right) H \\
& + iv^{-1} \left(-\rho^d m_d \bar{d}\gamma_5 d + \rho^u m_u \bar{u}\gamma_5 u - \rho^\ell m_\ell \bar{\ell}\gamma_5 \ell \right) A,
\end{aligned} \tag{2.3}$$

where ρ^X factors are given in table 3. Different types of the 2HDM show different character-

	I	II	X	Y
ρ^d	$\cot \beta$	$-\tan \beta$	$\cot \beta$	$-\tan \beta$
ρ^u	$\cot \beta$	$\cot \beta$	$\cot \beta$	$\cot \beta$
ρ^ℓ	$\cot \beta$	$-\tan \beta$	$-\tan \beta$	$\cot \beta$

Table 3: ρ^X factors of the neutral Higgs part of the Yukawa Lagrangian corresponding to different types.

istics [18] due to the difference among the factors. As table 3 shows, factors corresponding to the Type-I 2HDM increase as $\tan \beta$ decreases. Such a behaviour is one of the motivations behind working in low $\tan \beta$ regime in the context of this type.

3 Signal process

The signal process is assumed to be $e^-e^+ \rightarrow AH$ in the context of the 2HDM Type-I. The Higgs bosons are selected with different masses to provide possibility of $A \rightarrow ZH$ decay. Scenarios with equal masses were studied earlier leading to promising results under the same collider conditions [21]. The two scalar Higgs bosons then decay like $H \rightarrow b\bar{b}$ which is dominated in 2HDM Type-I and the Z boson undergoes $Z \rightarrow \ell\bar{\ell}$ decay where $\ell\bar{\ell}$ is an electron or a muon pair and b is the bottom quark. The center-of-mass energy of $\sqrt{s} = 1$ TeV is assumed for the initial collision at a linear collider. Two benchmark points with different mass hypotheses are assumed as shown in table 4. The physical mass of the H Higgs boson is assumed to take values 150 and 200 GeV, and the mass splitting between H and A Higgs bosons is assumed to be 100 GeV for on-shell Z boson production. The chosen Higgs boson masses are checked to be consistent with results of 86 analyses with the use of `HiggsBounds 4.3.1` [22] and `HiggsSignals 1.3.0` [23]. The value of $\tan \beta$ is also set to 10 for both benchmark points. For each scenario there is a range of m_{12}^2 parameter (quoted in Tab. 4) which satisfies theoretical requirements of potential stability [24], perturbativity and unitarity [25–28] which are all checked using `2HDMC 1.7.0` [29, 30].

Masses of the Higgs bosons A and H^\pm are assumed to be equal for both of the benchmark points to make sure that the experimental constraint [31, 32] is satisfied. This experimental constraint resulted from the measurement performed at LEP [33] and puts a limit on the deviation of the parameter $\rho = m_W^2(m_Z \cos \theta_W)^{-2}$ from its standard model

	BP1	BP2
m_h		125
m_H	150	200
m_A	250	300
m_{H^\pm}	250	300
m_{12}^2	2001-2223	3722-3972
$\tan\beta$		10
$\sin(\beta - \alpha)$		1

Table 4: Assumed benchmark points. m_H, m_h, m_A, m_{H^\pm} are physical masses of the Higgs bosons. The m_{12}^2 range satisfying theoretical requirements is provided for each scenario.

value. Since it is demonstrated that the deviation of this parameter is negligible if any of the conditions [34, 35]

$$m_A = m_{H^\pm}, \quad m_H = m_{H^\pm}, \quad (3.1)$$

is satisfied, the assumed benchmark points are guaranteed to be consistent with the mentioned experimental constraint. Flavor physics data constrains charged Higgs mass by the limit $m_{H^\pm} > 480$ GeV in the Type-II and Type-Y 2HDM [36, 37]. However, since the charged Higgs coupling to quarks in the Type-I 2HDM depends on $\cot\beta$ and differs from the same coupling in the Type-II and Type-Y 2HDM, the mentioned constraint does not limit choice of charged Higgs mass in this study. The assumed benchmark points are totally consistent with the results of ATLAS direct investigation [38] on 2HDM. Moreover, as indicated in [39–41], the limits $m_A \geq 93.4$ GeV and $m_{H^\pm} \geq 78.6$ GeV are already satisfied by the current analysis. The LHC experiments have recently excluded the region $m_{A/H} = 200 - 400$ GeV for $\tan\beta \geq 5$ [42, 43]. However, since the Type-I 2HDM differs considerably from the MSSM in structure, mass hypotheses in this study are not required to satisfy these conditions. Therefore, it can be concluded that the assumed benchmark points satisfy all of the theoretical and experimental constraints and can be used to generate signal events.

According to the full Lagrangian of the Type-I 2HDM, the Z - H - A vertex depends on $\sin(\beta - \alpha)$ which is assumed to be unity in the SM-like scenario. This vertex appears both in the production process, i.e., $e^+e^- \rightarrow Z^* \rightarrow HA$ and the subsequent decay $A \rightarrow ZH$. Therefore the production process followed by $A \rightarrow ZH$ decay is independent of $\tan\beta$ as long as $\sin(\beta - \alpha) = 1$. We obtain $\text{BR}(A \rightarrow ZH) \simeq 0.998$ and $\text{BR}(H \rightarrow b\bar{b}) \simeq 0.71$ for the two benchmark scenarios using 2HDMC 1.7.0. According to the signal process, the produced Z boson annihilates into a lepton pair ($\mu^-\mu^+$ or e^-e^+). Branching ratio of this decay mode (≈ 0.066) is so small compared with the hadronic decay mode. Despite this fact, the leptonic decay is chosen since leptons provide a simple and clear signature at linear colliders and this feature can compensate for the smallness of the branching ratio. Each signal event results in two H Higgs bosons which are assumed to decay into b quark pairs. The resulting b quarks annihilate into hadronic jets which are used to reconstruct the Higgs

boson. Reconstruction of the H and Z bosons is then followed by A reconstruction as fully discussed in the following sections.

Table 5 shows signal process cross section corresponding to the assumed benchmark points obtained by PYTHIA 8.2.15 [44]. As seen, the benchmark point with heavier Higgs

	BP1	BP2
Signal cross section [fb]	0.338	0.207

Table 5: Cross section of the signal process assuming different benchmark points.

masses corresponds to the smaller cross section. Therefore, observing the heavier Higgs boson is expected to be more difficult. Background processes contributing to this analysis include top quark pair production, W^\pm pair production, Z pair production and Z/γ production. Cross sections corresponding to the background processes are also obtained by PYTHIA 8.2.15 and are provided in Tab. 6.

	$t\bar{t}$	W^+W^-	ZZ	Z/γ
Cross section [fb]	211.1	3163	234.7	4335

Table 6: Background cross sections.

4 Analysis

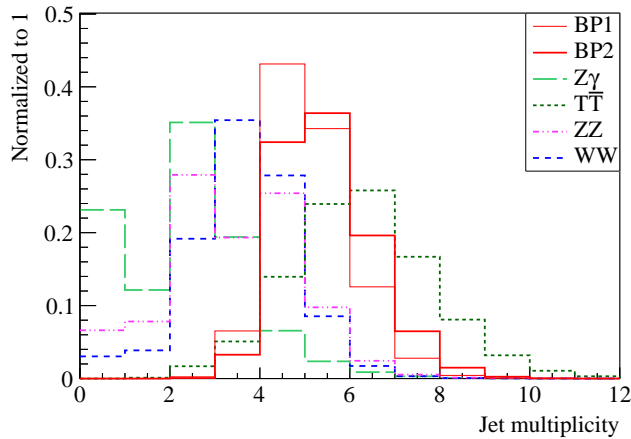
To generate signal events, basic parameters of the model are generated in SLHA (SUSY Les Houches Accord) format by 2HDMC 1.7.0 and the output is passed to PYTHIA 8.2.15 for event generation. Background events are also generated by PYTHIA 8.2.15. Based on the characteristics of the signal and background events, appropriate event selection cuts are applied to enrich signal events. FASTJET 3.1.0 [45, 46] is used to perform jet reconstruction. According to properties of the jets, anti- k_t algorithm [47] with the cone size $\Delta R = \sqrt{(\Delta\eta)^2 + (\Delta\phi)^2} = 0.4$ is employed. Here, $\eta = -\ln \tan(\theta/2)$ and ϕ (θ) is the azimuthal (polar) angle with respect to the beam axis. After jets are identified, jet energy smearing is applied to jets according to energy resolution $\sigma/E = 3.5\%$ [48]. Jets are required to satisfy the conditions

$$p_{Tjet} \geq 10 \text{ GeV}, \quad |\eta_{jet}| \leq 4, \quad (4.1)$$

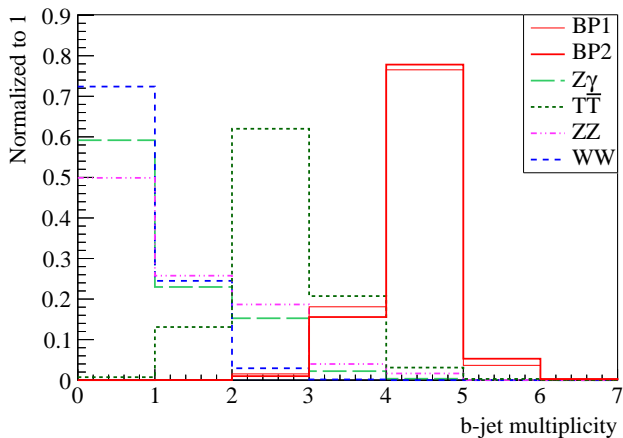
where p_T is the transverse momentum. Counting jets in each event results in jet multiplicity distributions as shown in Fig. 1(a). Based on the obtained distributions, the condition

$$N_{jet} \geq 4, \quad (4.2)$$

is applied, where N_{jet} is the number of jets. Applying the b -tagging algorithm to jets, the b -jet multiplicity distributions are obtained as shown in Fig. 1(b). The b -tagging method



(a)



(b)

Figure 1: a) Jet multiplicity and b) b -jet multiplicity obtained for signal and background processes.

is based on b -tag efficiency, c -jets mis-tag rate and light jets mis-tag rate assumed to be 0.7, 0.07 and 0.003 respectively [48]. Based on the distributions of Fig. 1(b), the selection cut

$$N_{b\text{-jet}} \geq 3. \quad (4.3)$$

is applied to include events with at least three b -jets.

Leptons (electrons and muons) present in the events are identified and momentum smearing according to the momentum resolution $\sigma_{p_T}/p_T^2 = 2 \times 10^{-5} \text{ GeV}^{-1}$ [48] is applied to them. Counting the number of electrons and muons which satisfy the conditions

$$p_{T_{e,\mu}} \geq 5 \text{ GeV}, \quad |\eta_{e,\mu}| \leq 4, \quad (4.4)$$

the number of di-leptons is obtained. A di-lepton can be a di-electron or a di-muon. Figure 2 shows the obtained di-lepton multiplicity corresponding to different processes. The selection

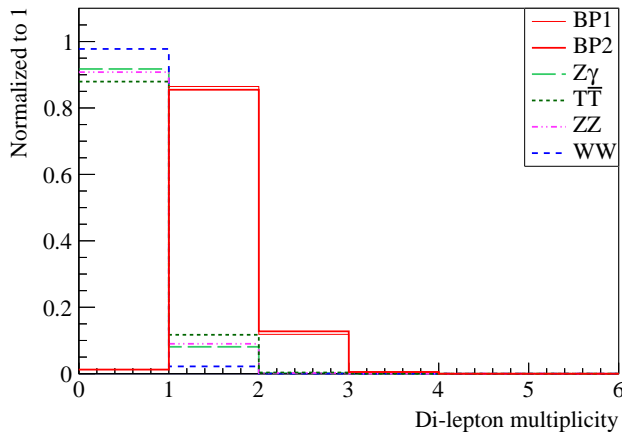


Figure 2: Di-lepton multiplicity distributions of the signal and background events.

cut

$$N_{\ell\bar{\ell}} \geq 1, \quad (4.5)$$

where $N_{\ell\bar{\ell}}$ is the number of di-leptons, is now applied to rule out events with no di-lepton.

Events with at least one di-lepton are then subject to conditions

$$60 \leq I.M._{\ell\bar{\ell}} \leq 100 \text{ GeV}, \quad (4.6)$$

where $I.M._{\ell\bar{\ell}}$ is the invariant mass of the di-lepton. An event is selected if it has a di-lepton satisfying these conditions.

Analyzing the b -tagged jets, decay products of the H Higgs bosons are identified. In each event, the parameter

$$\Delta R = \sqrt{(\Delta\eta)^2 + (\Delta\phi)^2}, \quad (4.7)$$

is computed for all possible b -jet pairs and the pair for which the ΔR value is minimized, is identified as the true pair which originates from the H Higgs boson. Computing the invariant masses of the identified true b -jet pairs, H Higgs mass is reconstructed and a mass distribution is obtained as fully discussed later.

Having reconstructed the H Higgs boson, another selection cut is applied to events and then the A Higgs boson mass will be reconstructed. Events which satisfy any of the conditions

$$\begin{aligned} N_{b\bar{b}} &\geq 2, \\ \Delta R(ZH) &\leq 1 \quad (\text{if } N_{b\bar{b}} = 1), \end{aligned} \quad (4.8)$$

where $N_{b\bar{b}}$ is the number of identified true b -jet pairs, pass the selection cut. $\Delta R(ZH)$ is the spatial distance (defined by Eq. 4.7) between the reconstructed H boson (originating from the b -jet pair) and the reconstructed Z boson (originating from the di-lepton). Therefore, events with two or more true b -jet pairs, and events with one true b -jet pair which satisfy $\Delta R(ZH) \leq 1$, survive the last selection cut.

In events with one b -jet pair, computing the invariant mass of the b -jet pair and the lepton pair results in a value for the mass of A boson. In events with two b -jet pairs, the

b -jet pair which its corresponding reconstructed H boson has smaller spatial distance (see Eq. 4.7) from the reconstructed Z boson (originating from the di-lepton) is identified as the decay product of the A Higgs boson. In such events also a value for the A boson mass is obtained as the invariant mass of the identified b -jet pair and the lepton pair.

Event selection efficiencies corresponding to the applied selection cuts are provided in tables 7 and 8. H and A candidate mass distributions are obtained after four and five cuts respectively. Total efficiencies corresponding to the first four cuts and all the five cuts are also provided.

	BP1	BP2
$N_{jet} \geq 4$	0.932	0.967
$N_{b-jet} \geq 3$	0.984	0.990
$N_{\ell\bar{\ell}} \geq 1$	0.988	0.988
$60 \leq I.M._{\ell\bar{\ell}} \leq 100$	0.880	0.864
Total eff.	0.797	0.817
$\Delta R(ZH) \leq 1$	0.913	0.922
Total eff.	0.728	0.753

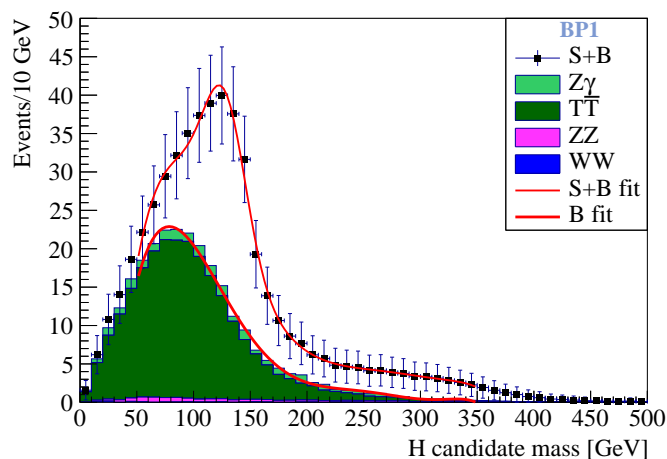
Table 7: Event selection efficiencies corresponding to the signal process assuming two benchmark points.

	$t\bar{t}$	WW	ZZ	$Z\gamma$
$N_{jet} \geq 4$	0.93117	0.38491	0.38328	0.10204
$N_{b-jet} \geq 3$	0.24171	0.00172	0.05706	0.02581
$N_{\ell\bar{\ell}} \geq 1$	0.12008	0.02146	0.09049	0.08195
$60 \leq I.M._{\ell\bar{\ell}} \leq 100$	0.07854	0.05634	0.03264	0.03429
Total eff.	2.12e-03	8e-07	6e-05	7.4e-06
$\Delta R(ZH) \leq 1$	0.33955	0.25000	0.61610	0.54054
Total eff.	7.2e-04	2e-07	4e-05	4e-06

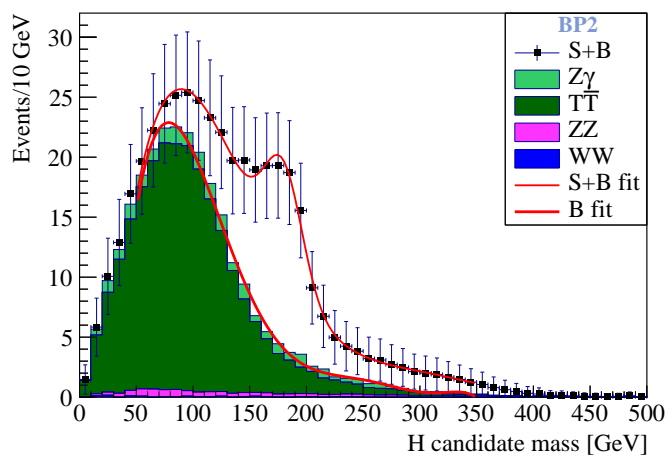
Table 8: Event selection efficiencies corresponding to background processes.

5 Higgs boson reconstruction

Computing candidate masses of the H and A Higgs bosons as explained, mass distributions of Figs. 3 and 4 are obtained. Contributions of the signal and different background



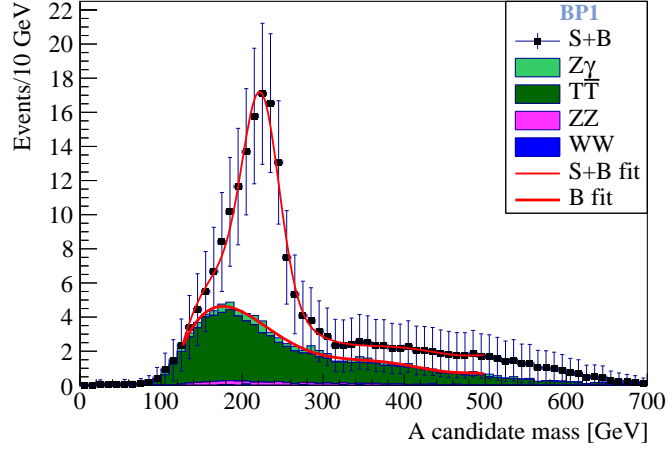
(a)



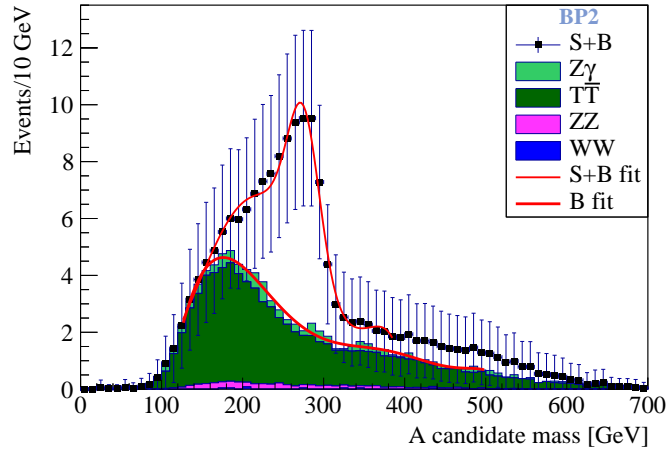
(b)

Figure 3: H candidate mass distributions with corresponding fitting results assuming the benchmark points a) BP1 and b) BP2 at the integrated luminosity of 500 fb^{-1} . Statistical errors are also shown.

processes are shown separately and the signal contribution can be seen as a significant excess of data on top of the standard model background. The WW process has the least contribution because of the perfect suppression due to the second and third selection cuts as seen in table 8. Normalization of the distributions is based on $L \times \sigma \times \epsilon$, where L is the integrated luminosity which is assumed to be 500 fb^{-1} , σ is the cross section which is taken from tables 5 and 6, and ϵ is the total efficiency. Total efficiencies used for normalizing A mass distributions are taken from the last rows of tables 7 and 8. However, total efficiencies corresponding to the first four selection cuts of tables 7 and 8 cannot be used to normalize H mass distributions since the number of reconstructed H Higgs bosons in events surviving



(a)



(b)

Figure 4: A candidate mass distributions with corresponding fitting results assuming the benchmark points a) BP1 and b) BP2 at the integrated luminosity of 500 fb^{-1} . Statistical errors are also shown.

the cuts is different from event to event. Therefore, total efficiencies $\epsilon_{BP1} = 0.72$ and $\epsilon_{BP2} = 0.75$ obtained by counting the number of reconstructed H Higgs bosons, are used for normalizing H mass signal distributions and total efficiencies $\epsilon_{t\bar{t}} = 2.2e - 03$, $\epsilon_{WW} = 8.3e - 07$, $\epsilon_{ZZ} = 8.8e - 05$ and $\epsilon_{Z\gamma} = 1.1e - 05$ are used to normalize background contributions. Benchmark points BP1 and BP2 correspond to Higgs generated masses $m_H = 150$ and 200 , and $m_A = 250$ and 300 GeV respectively. As seen in Figs. 3 and 4, candidate mass distributions have significant peaks near the generated masses.

Fitting results of the signal plus background and background distributions are also shown in Figs. 3 and 4. Fitting results are obtained by ROOT 5.34 [49] and the fit function

used for the signal plus background distribution is a combination of the polynomial and gaussian functions. A polynomial function is first used as the fit function for the total background distribution and is then used as input for the total signal plus background fit. The Higgs boson reconstructed masses can be read from the “mean” parameter of the Gaussian function assumed as the signal distribution function.

Obtaining values of the “Mean” parameter, reconstructed masses of the Higgs bosons H and A are found and provided in table 9. The difference between generated and

		BP1	BP2
H	Gen. mass [GeV]	150	200
	Rec. mass [GeV]	127.84±4.64	180.03±6.51
A	Gen. mass [GeV]	250	300
	Rec. mass [GeV]	223.24±4.72	275.23±8.44

Table 9: Reconstructed and generated masses of H and A Higgs bosons with associated uncertainties.

		BP1	BP2
H	Gen. mass [GeV]	150	200
	Corr. rec. mass [GeV]	148.91±10.22	201.1±12.09
A	Gen. mass [GeV]	250	300
	Corr. rec. mass [GeV]	249.01±11.3	301±15.02

Table 10: Corrected reconstructed masses of H and A Higgs bosons with associated uncertainties.

reconstructed masses of table 9 can be due to the uncertainty arising from fitting method and choice of the fit function, jet reconstruction algorithm and jet mis-identification, b -tagging algorithm and jets mis-tag rate and also the errors in energy and momentum of the particles, etc. Optimization of the b -tagging algorithm, fitting method and also optimization of the jet reconstruction algorithm using MC truth matching tools can reduce the errors in the reconstructed masses. In addition to the mentioned error sources, electronic noise, pile up, underlying-events, etc, can give rise to more errors in obtained reconstructed masses in case of real experiments, and thus a careful correction must be applied.

Since the mentioned corrections lie beyond the scope of this paper, a simple off-set correction is applied to the obtained reconstructed masses as follows. On average, reconstructed masses of the H and A Higgs bosons are 21.07 and 25.77 GeV smaller than the corresponding generated masses respectively. To apply the off-set correction, reconstructed

masses of the H and A Higgs bosons are increased by the same values respectively. Table 10 provides the corrected reconstructed masses of the Higgs bosons. The errors are statistical but include also sources of uncertainties from the jet and track energy and momentum resolutions assumed in the analysis.

6 Signal significance

Using the Higgs candidate mass distributions of Figs. 3 and 4, signal significance is obtained to assess the observability of the Higgs bosons. A mass window cut is applied to distributions and the signal significance is computed by counting signal and background events which pass the mass window. The mass window is determined by maximizing the signal significance. The integrated luminosity at which computation is performed is set to 500 fb^{-1} . However, it is indicated that the Higgs bosons are also observable at lower luminosities. The minimum required integrated luminosities at which the Higgs bosons are observable with 5σ signals are also computed and provided as “ 5σ integrated \mathcal{L} .”. Table 11 provides computation results, namely mass window and the corresponding efficiency, signal selection total efficiency, number of signal (S) and background (B) Higgs candidates which pass the mass window, signal to background ratio, signal significance and 5σ integrated luminosity. According to the results, it is indicated that for both of the benchmark points, both of the Higgs bosons H and A are observable with signals exceeding 5σ at the integrated luminosity of 500 fb^{-1} and the minimum required integrated luminosity at which the Higgs boson H (A) is observable is 46 (112) fb^{-1} . Mass measurement is also possible for both of the Higgs bosons. As seen, minimum required integrated luminosity for observing the heavier Higgs boson is higher. This is because of the fact that cross section of the Higgs production varies inversely as the Higgs mass.

7 Conclusions

The signal process chain $e^-e^+ \rightarrow AH \rightarrow ZHH \rightarrow \ell\bar{\ell}b\bar{b}b\bar{b}$, where $\ell\bar{\ell}$ is a di-electron or a di-muon, was investigated to assess the observability of the CP-even (H) and CP-odd (A) Higgs bosons in the framework of the Type-I 2HDM at SM-like scenario. Electron-positron annihilation is assumed to occur at the center-of-mass energy of $\sqrt{s} = 1 \text{ TeV}$ at a linear collider. The signal benefits from large enhancements due to the decay modes $A \rightarrow ZH$ and $H \rightarrow b\bar{b}$ at a relatively low $\tan\beta$ value. The leptonic decay $Z \rightarrow \ell\bar{\ell}$ is assumed to benefit from the clear signature of leptons at lepton colliders. Two benchmark points with different mass hypotheses in the parameter space of the Type-I 2HDM were simulated and analysed with the help of characteristics of the signal and background events and appropriate selection cuts. Physical mass of the Higgs boson H (A) is assumed to vary in range 150-200 GeV (250-300 GeV). Jet energy smearing was performed according to the energy resolution $\sigma/E = 3.5\%$. Momentum smearing was also applied to leptons according to the momentum resolution $\sigma_{p_T}/p_T^2 = 2 \times 10^{-5} \text{ GeV}^{-1}$. Higgs candidate mass distributions corresponding to assumed benchmark points were obtained and reconstructed masses of the Higgs bosons were obtained by fitting an appropriate fit function to mass distributions and

		BP1	BP2
H	Gen. mass [GeV]	150	200
	Mass window [GeV]	>109	>147
	Mass window cut eff.	0.76	0.70
	Total eff.	0.546	0.530
	S	184.7	108.9
	B	96.8	43.2
	S/B	1.9	2.5
	S/\sqrt{B}	18.8	16.6
	Integrated \mathcal{L} [fb^{-1}]	500	
	5σ integrated \mathcal{L} [fb^{-1}]	36	46
A	Gen. mass [GeV]	250	300
	Mass window [GeV]	191-264	232-304
	Mass window cut eff.	0.58	0.56
	Total eff.	0.42	0.42
	S	71.2	43.6
	B	25.3	17.0
	S/B	2.8	2.6
	S/\sqrt{B}	14.2	10.6
	Integrated \mathcal{L} [fb^{-1}]	500	
	5σ integrated \mathcal{L} [fb^{-1}]	63	112

Table 11: Generated mass, optimized mass window cut and associated efficiency, signal total efficiency, number of signal and background Higgs candidates after all cuts, signal to background ratio, signal significance, assumed integrated luminosity, and the integrated luminosity at which the Higgs boson is observable with a 5σ signal (5σ integrated \mathcal{L}).

then extracting the value of the “mean” parameter of the gaussian fit function. Signal significance was also computed to assess observability of the Higgs bosons. Results indicate that for both of the assumed benchmark points, Higgs bosons H and A are observable with signals exceeding 5σ at the integrated luminosity of $500 fb^{-1}$. Mass measurement is also possible for both of the Higgs bosons. Moreover, it was shown that the minimum required integrated luminosities at which the Higgs bosons H and A are observable are 46 and 112 fb^{-1} respectively. Since such luminosities are accessible to future linear colliders, this study is expected to serve experimentalists well in search for Higgs bosons in the context of 2HDM.

Acknowledgements

The analysis presented in this work was fully performed using the computing cluster at Shiraz University, college of sciences. We would like to thank Dr. Mogharrab for his careful maintenance and operation of the computing cluster.

References

- [1] F. Englert and R. Brout, *Broken Symmetry and the Mass of Gauge Vector Mesons*, *Phys. Rev. Lett.* **13** (1964) 321–323.
- [2] P. W. Higgs, *Broken Symmetries and the Masses of Gauge Bosons*, *Phys. Rev. Lett.* **13** (1964) 508–509.
- [3] P. W. Higgs, *Broken symmetries, massless particles and gauge fields*, *Phys. Lett.* **12** (1964) 132–133.
- [4] G. S. Guralnik, C. R. Hagen, and T. W. B. Kibble, *Global Conservation Laws and Massless Particles*, *Phys. Rev. Lett.* **13** (1964) 585–587.
- [5] P. W. Higgs, *Spontaneous Symmetry Breakdown without Massless Bosons*, *Phys. Rev.* **145** (1966) 1156–1163.
- [6] T. W. B. Kibble, *Symmetry breaking in nonAbelian gauge theories*, *Phys. Rev.* **155** (1967) 1554–1561.
- [7] CMS Collaboration, S. Chatrchyan et al., *Observation of a new boson at a mass of 125 GeV with the CMS experiment at the LHC*, *Phys. Lett.* **B716** (2012) 30–61, [[arXiv:1207.7235](#)].
- [8] ATLAS Collaboration, G. Aad et al., *Observation of a new particle in the search for the Standard Model Higgs boson with the ATLAS detector at the LHC*, *Phys. Lett.* **B716** (2012) 1–29, [[arXiv:1207.7214](#)].
- [9] I. J. R. Aitchison, *Supersymmetry and the MSSM: An Elementary introduction*, [hep-ph/0505105](#).
- [10] J. E. Kim, *Light pseudoscalars, particle physics and cosmology*, *Physics Reports* **150** (1987), no. 1 1 – 177.
- [11] M. Trodden, *Electroweak baryogenesis: A Brief review*, in *Proceedings, 33rd Rencontres de Moriond 98 electroweak interactions and unified theories: Les Arcs, France, Mar 14-21, 1998*, pp. 471–480, 1998. [hep-ph/9805252](#).
- [12] G. C. Branco, P. M. Ferreira, L. Lavoura, M. N. Rebelo, M. Sher, and J. P. Silva, *Theory and phenomenology of two-Higgs-doublet models*, *Phys. Rept.* **516** (2012) 1–102, [[arXiv:1106.0034](#)].
- [13] T. D. Lee, *A Theory of Spontaneous T Violation*, *Phys. Rev.* **D8** (1973) 1226–1239.
- [14] S. L. Glashow and S. Weinberg, *Natural Conservation Laws for Neutral Currents*, *Phys. Rev.* **D15** (1977) 1958.
- [15] G. C. Branco, *Spontaneous CP Nonconservation and Natural Flavor Conservation: A Minimal Model*, *Phys. Rev.* **D22** (1980) 2901.
- [16] J. Mrazek, A. Pomarol, R. Rattazzi, M. Redi, J. Serra, and A. Wulzer, *The Other Natural Two Higgs Doublet Model*, *Nucl. Phys.* **B853** (2011) 1–48, [[arXiv:1105.5403](#)].

- [17] S. Davidson and H. E. Haber, *Basis-independent methods for the two-Higgs-doublet model*, *Phys. Rev.* **D72** (2005) 035004, [[hep-ph/0504050](#)]. [Erratum: *Phys. Rev.*D72,099902(2005)].
- [18] M. Aoki, S. Kanemura, K. Tsumura, and K. Yagyu, *Models of Yukawa interaction in the two Higgs doublet model, and their collider phenomenology*, *Phys. Rev.* **D80** (2009) 015017, [[arXiv:0902.4665](#)].
- [19] M. D. Campos, D. Cogollo, M. Lindner, T. Melo, F. S. Queiroz, and W. Rodejohann, *Neutrino Masses and Absence of Flavor Changing Interactions in the 2HDM from Gauge Principles*, *JHEP* **08** (2017) 092, [[arXiv:1705.05388](#)].
- [20] V. D. Barger, J. L. Hewett, and R. J. N. Phillips, *New Constraints on the Charged Higgs Sector in Two Higgs Doublet Models*, *Phys. Rev.* **D41** (1990) 3421–3441.
- [21] M. Hashemi and M. MahdaviKhorrani, *Analysis of b quark pair production signal from neutral 2HDM Higgs bosons at future Linear Colliders*, [arXiv:1804.10790](#).
- [22] P. Bechtle, O. Brein, S. Heinemeyer, O. Stål, T. Stefaniak, G. Weiglein, and K. E. Williams, *HiggsBounds – 4: Improved Tests of Extended Higgs Sectors against Exclusion Bounds from LEP, the Tevatron and the LHC*, *Eur. Phys. J.* **C74** (2014), no. 3 2693, [[arXiv:1311.0055](#)].
- [23] P. Bechtle, S. Heinemeyer, O. Stål, T. Stefaniak, and G. Weiglein, *HiggsSignals: Confronting arbitrary Higgs sectors with measurements at the Tevatron and the LHC*, *Eur. Phys. J.* **C74** (2014), no. 2 2711, [[arXiv:1305.1933](#)].
- [24] N. G. Deshpande and E. Ma, *Pattern of symmetry breaking with two higgs doublets*, *Phys. Rev. D* **18** (Oct, 1978) 2574–2576.
- [25] H. Hüffel and G. Pócsik, *Unitarity bounds on higgs boson masses in the weinberg-salam model with two higgs doublets*, *Zeitschrift für Physik C Particles and Fields* **8** (Mar, 1981) 13–15.
- [26] J. Maalampi, J. Sirkka, and I. Vilja, *Tree level unitarity and triviality bounds for two-higgs models*, *Physics Letters B* **265** (1991), no. 3 371 – 376.
- [27] S. Kanemura, K. Tsumura, and H. Yokoya, *Multi-tau-lepton signatures at the LHC in the two Higgs doublet model*, *Phys. Rev.* **D85** (2012) 095001, [[arXiv:1111.6089](#)].
- [28] A. G. Akeroyd, A. Arhrib, and E. Naimi, *Note on tree-level unitarity in the general two higgs doublet model*, *Physics Letters B* **490** (2000), no. 1 119 – 124.
- [29] D. Eriksson, J. Rathsman, and O. Stal, *2HDMC: Two-Higgs-Doublet Model Calculator Physics and Manual*, *Comput. Phys. Commun.* **181** (2010) 189–205, [[arXiv:0902.0851](#)].
- [30] D. Eriksson, J. Rathsman, and O. Stal, *2HDMC: Two-Higgs-doublet model calculator*, *Comput. Phys. Commun.* **181** (2010) 833–834.
- [31] S. Bertolini, *Quantum effects in a two higgs doublet model of the electroweak interactions*, *Nuclear Physics B* **272** (1986), no. 1 77 – 98.
- [32] A. Denner, R. Guth, and J. Kühn, *Relaxation of top mass limits in the two-higgs-doublet model*, *Physics Letters B* **240** (1990), no. 3 438 – 440.
- [33] W.-M. Y. et al, *Review of particle physics*, *Journal of Physics G: Nuclear and Particle Physics* **33** (2006), no. 1 1.
- [34] W. Grimus, L. Lavoura, O. M. Ogreid, and P. Osland, *A Precision constraint on multi-Higgs-doublet models*, *J. Phys.* **G35** (2008) 075001, [[arXiv:0711.4022](#)].
- [35] J. M. Gerard and M. Herquet, *A Twisted custodial symmetry in the two-Higgs-doublet model*, *Phys. Rev. Lett.* **98** (2007) 251802, [[hep-ph/0703051](#)].

- [36] M. Misiak et al., *Updated NNLO QCD predictions for the weak radiative B-meson decays*, *Phys. Rev. Lett.* **114** (2015), no. 22 221801, [[arXiv:1503.01789](#)].
- [37] M. Misiak and M. Steinhauser, *Weak radiative decays of the b meson and bounds on m_{H^\pm} in the two-higgs-doublet model*, *The European Physical Journal C* **77** (Mar, 2017) 201.
- [38] **ATLAS** Collaboration, G. Aad et al., *Search for an additional, heavy Higgs boson in the $H \rightarrow ZZ$ decay channel at $\sqrt{s} = 8$ TeV in pp collision data with the ATLAS detector*, *Eur. Phys. J.* **C76** (2016), no. 1 45, [[arXiv:1507.05930](#)].
- [39] **ALEPH** Collaboration, R. Barate et al., *Search for charged Higgs bosons in e^+e^- collisions at energies up to $\sqrt{s} = 189$ GeV*, *Phys. Lett.* **B487** (2000) 253–263, [[hep-ex/0008005](#)].
- [40] **L3** Collaboration, M. Acciarri et al., *Search for charged Higgs bosons in e^+e^- collisions at center center-of-mass energies up to 202-GeV*, *Phys. Lett.* **B496** (2000) 34–42, [[hep-ex/0009010](#)].
- [41] **DELPHI, OPAL, ALEPH, LEP Higgs Working Group, L3** Collaboration, *Searches for the neutral Higgs bosons of the MSSM: Preliminary combined results using LEP data collected at energies up to 209-GeV*, in *Lepton and photon interactions at high energies. Proceedings, 20th International Symposium, LP 2001, Rome, Italy, July 23-28, 2001*.
- [42] **CMS** Collaboration, *Search for a neutral MSSM Higgs boson decaying into $\tau\tau$ with 12.9 fb $^{-1}$ of data at $\sqrt{s} = 13$ TeV*, *CMS Collaboration, CMS-PAS-HIG-16-037*.
- [43] **ATLAS** Collaboration, *Search for Minimal Supersymmetric Standard Model Higgs bosons H/A in the $\tau\tau$ final state in up to 13.3 fb $^{-1}$ of pp collisions at $\sqrt{s} = 13$ TeV with the ATLAS Detector*, *The ATLAS Collaboration, ATLAS-CONF-2016-085*.
- [44] T. Sjöstrand, S. Ask, J. R. Christiansen, R. Corke, N. Desai, P. Ilten, S. Mrenna, S. Prestel, C. O. Rasmussen, and P. Z. Skands, *An introduction to pythia 8.2*, *Computer Physics Communications* **191** (2015) 159 – 177.
- [45] M. Cacciari, *FastJet: A Code for fast k_t clustering, and more*, in *Deep inelastic scattering. Proceedings, 14th International Workshop, DIS 2006, Tsukuba, Japan, April 20-24, 2006*, pp. 487–490, 2006. [[hep-ph/0607071](#)]. [,125(2006)].
- [46] M. Cacciari, G. P. Salam, and G. Soyez, *FastJet User Manual*, *Eur. Phys. J.* **C72** (2012) 1896, [[arXiv:1111.6097](#)].
- [47] M. Cacciari, G. P. Salam, and G. Soyez, *The Anti- $k(t)$ jet clustering algorithm*, *JHEP* **04** (2008) 063, [[arXiv:0802.1189](#)].
- [48] L. Linssen, A. Miyamoto, M. Stanitzki, and H. Weerts, *Physics and Detectors at CLIC: CLIC Conceptual Design Report*, [[arXiv:1202.5940](#)].
- [49] R. Brun and F. Rademakers, *ROOT: An object oriented data analysis framework*, *Nucl. Instrum. Meth.* **A389** (1997) 81–86.